ELECTRON-LATTICE INTERACTION AND NONLINEAR EXCITATIONS IN CUPRATE STRUCTURES

J. PAULSEN, H. ESCHRIG
MPG-Arbeitsgruppe Elektronensysteme
TU Dresden, D-01062 Dresden, Germany

S.-L. DRECHSLER and J. MALEK
Institut für Festkörper- und Werkstofforschung Dresden e.V.
Postfach, D-01171 Dresden, Germany

ABSTRACT

A low temperature lattice modulation of the chains of the $YBa_2Cu_3O_7$ is considered by deriving a Hamiltonian of electron-lattice interaction from density-functional calculations for deformed lattices and solving it for the groundstate. Hubbard-type Coulomb interaction is included. The obtained groundstate is a charge-density-wave state with a periodicity of four lattice constants and a gap for one-electron excitations of about 1eV, sensitively depending on parameters of the Hamiltonian. There are lots of polaronic and solitonic excitations with formation energies deep in the gap, which can pin the Fermi level and thus produce again metallicity of the chain. They might also contribute to pairing of holes in adjacent CuO_2-planes.

1. Introduction

Treating in mean field approximation a Holstein type model Hamiltonian with reasonable assumptions on the deformation potentials for chain states of $YBa_2Cu_3O_7$, a charge density wave (CDW) groundstate of the chains was predicted some time ago [1]. In the present work, the model is refined and extented to include Coulomb correlations. A great number of deformation potentials have been determined by density-functional calculations. The treatment of the model is improved by using Hartree-Fock theory plus many-body perturbation theory. This has been checked by direct diagonalization for short chains to give correct results. The previous results for the CDW state and the low-energy polaronic excitations are confirmed. The CDW groundstate was recently directly seen experimentally [2].

In subsequent sections, the electron count for the chain is considered, then the model is introduced in three steps: first a tight-binding fit for the undistorted chain is found, second the deformation potentials are determined, and finally screened Coulomb correlation terms—again provided with deformation potentials—are added. The model is solved by minimizing the total energy, and results are given.

2. Electron Count in $YBa_2Cu_3O_7$

The stacking sequence of the unit cell of $YBa_2Cu_3O_7$ in c-direction is as follows:

cationic sheet	Y^{+3}
metallic plane	$[CuO_2]^{-2+\delta}$
cationic sheet	Ba^{+2}
metallic chains	$[CuO_3]^{-3-2\delta}$
cationic sheet	Ba^{+2}
metallic plane	$[CuO_2]^{-2+\delta}$

δ is the number of holes per unit cell in one CuO_2-plane. Experimentally it is close to 0.25 [3]. If in the CuO_3-radical of the chains all Cu($3d$)-states and all O($2p$)-states were occupied, a $[CuO_3]^{-5}$-layer would result. At the top of the Cu($3d$)-O($2p$)-band complex, a single antibonding band is nearly separated, which can hold two electrons per unit cell (one per spin), if it is not split by correlation. In order to get a $[CuO_3]^{-3-2\delta}$ situation, this band must be occupied by 2δ electrons, which number is experimentally close to 0.5. This means that on average only every second unit cell is occupied with one electron in this band, and hence the band is expected to be quarterly filled and only weakly correlated (in contrast to the half-filled—with one electron per unit cell—strongly correlated plane-band of $YBa_2Cu_3O_6$).

3. Electronic Chain Model

The singled out antibonding Cu($3d$)-O($2p$)-band of the chains hybridizes only very weakly with other orbitals in the structure. Fig. 1 shows the relevant orbitals of the chain. The chain band of interest is the upper band of the 2×2 Hamiltonian matrix

$$(\hat{H}) = \begin{pmatrix} E_1 & 2T\sin k \\ 2T\sin k & E_2 \end{pmatrix}, \tag{1}$$

i.e., the band

$$\varepsilon(k) = \bar{E} + \sqrt{\Delta^2/4 + (2T\sin k)^2}, \quad \bar{E} = (E_1 + E_2)/2, \quad \Delta = E_1 - E_2. \tag{2}$$

All-electron selfconsistent density-functional calculations yield a width of this band of 2.5 eV. With the simple model (2) we were able to fit the result of such an all-electron calculation within 0.04 eV (maximal deviation).

Our aim is to study electron-lattice interaction. To this goal we consider displacements u_i^ν of type ν related to the chain site i. ν may, e.g., denote a direction for the chain oxygen atom or an internal molecular mode of the CuO_2 radical formed with the apical oxygens, or even a displacement of another atom off the chain. We

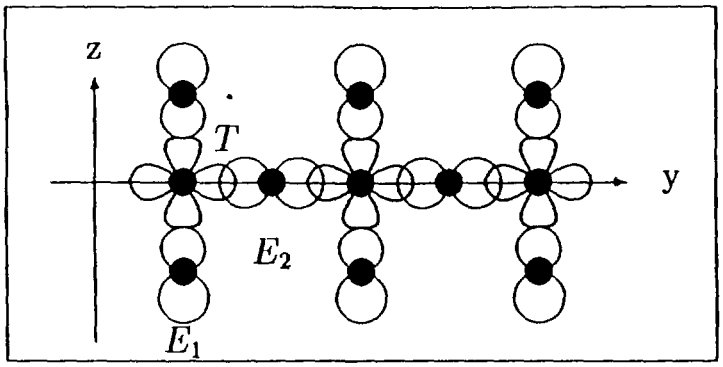

Figure 1: Orbitals of the chain band model. E_1 is the orbital energy of the anti-bonding CuO_2 molecular orbital of the chain-Cu and the two apex oxygens, E_2 is the orbital energy of the chain oxygen, and T is the transfer matrix element between both orbitals.

generalize the Hamiltonian (1) into a Holstein-type Hamiltonian

$$\hat{H} = \sum_i \left[E_i \hat{c}_i^\dagger \hat{c}_i - T_{i,i+1}(\hat{c}_i^\dagger \hat{c}_{i+1} + \hat{c}_{i+1}^\dagger \hat{c}_i) \right], \tag{3}$$

$$E_i = E_i^0 + \sum_\nu \alpha_\nu u_i^\nu, \quad T_{ij} = T_{ij}^0 + \sum_\nu \left(\gamma_\nu u_i^\nu + \gamma'_\nu u_j^\nu \right) \tag{4}$$

with deformation potentials α_ν and γ_ν, γ'_ν.

4. Deformation Potentials

In order to obtain reliable deformation potentials (4) for the real solid, and also to get a better understanding on what are the relevant lattice modes, we performed independent all-electron selfconsistent density-functional calculations for quite a number of frozen in zone center and zone boundary displacive modes. For each displacement pattern, the resulting bands originating from the band (2) of the undistorted structure were fitted with our tight-binding model parameters (4). In order to track possible changes in hybridization with other orbitals when the symmetry of the lattice is lowered, we used an all-electron LCAO scheme for the density-functional calculations, which gave reasonable agreement with full-potential results [4]—particularly with respect to the considered chain band—, but yielded directly projections on atomic orbitals for all band states. The quality of the tight-binding fits for the energies was in all cases as reported in the previous section, although the fit was not always quite unique for the matrix elements E_1, E_2 and T.

Results of such density-functional calculations of deformation potentials are given on Fig. 2a-e for zone-center modes, and on Fig. 3a-c for zone-boundary modes. The deformation dependence shown on Fig. 2a agrees with a previous independent calculation [5]. Note in Fig. 3 the large gap in the upper chain band produced by quite small displacements of the oxygen atoms of the chain.

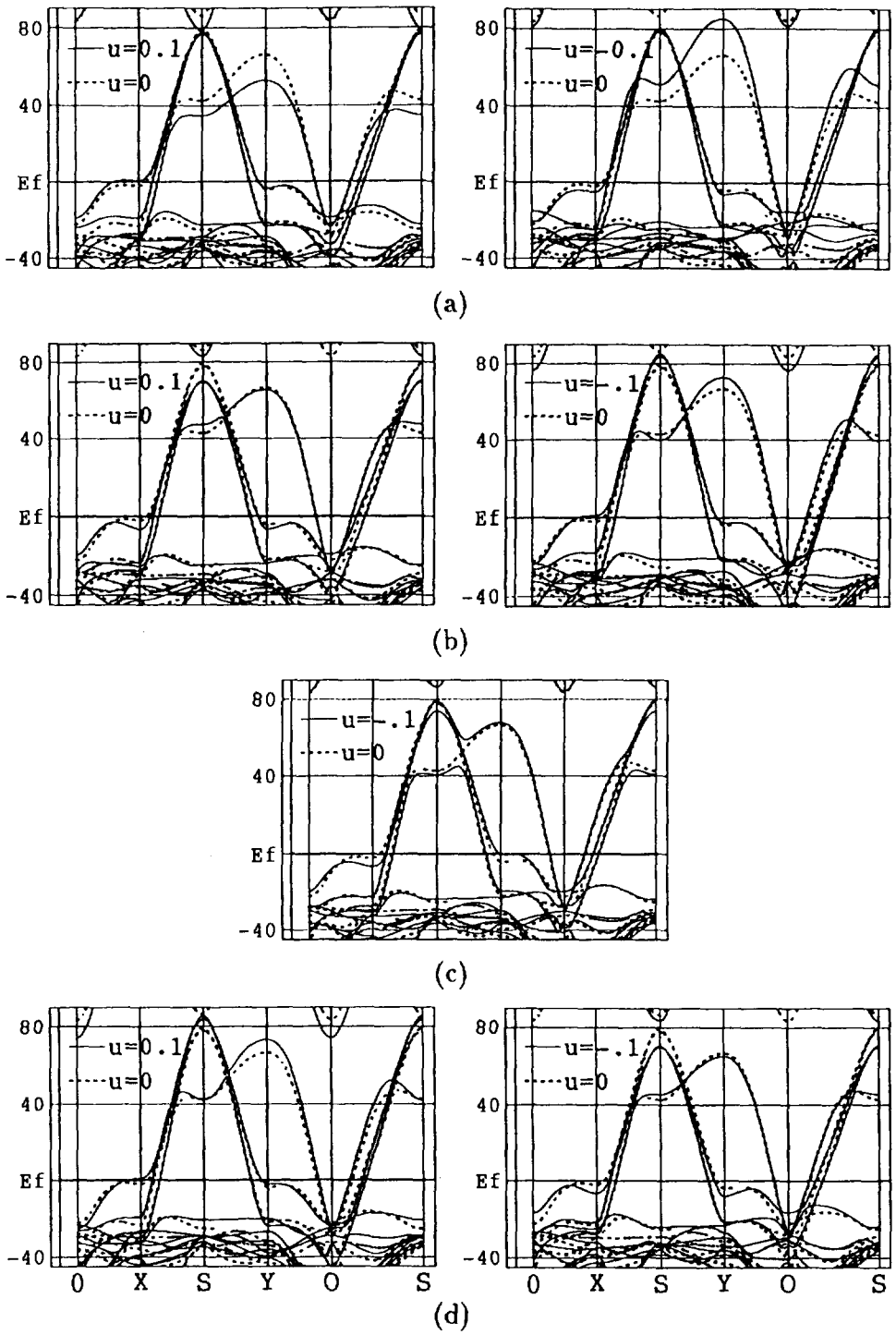

Figure 2: Band structure of $YBa_2Cu_3O_7$ in dependence of various zone-center displacements of atoms. The bands of the undisplaced lattice are given in dashed lines on all panels. Energies are given in mHartree units, displacements in Å.

a) Symmetric apex oxygen displacement in z-direction, u is the change in oxygen-oxygen distance.

b) In phase displacement of plane oxygen O(2) and O(3) in z-direction, u is the increase of the distance between planes across the chain.

c) Antiphase displacement of plane oxygens in z-direction.

d) Plane-Cu displacement in z-direction, u is the increase of the distance between planes across the chain.

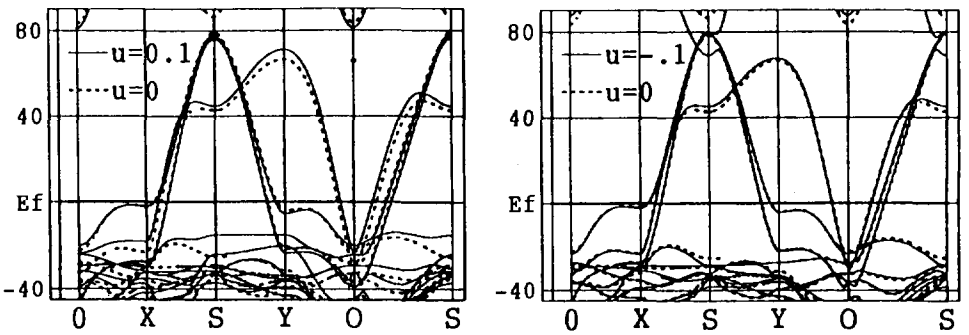

(e)

Figure 2: Continuation.
e) Ba displacement in z-direction, u is the increase of the Ba–Ba distance across the chain.

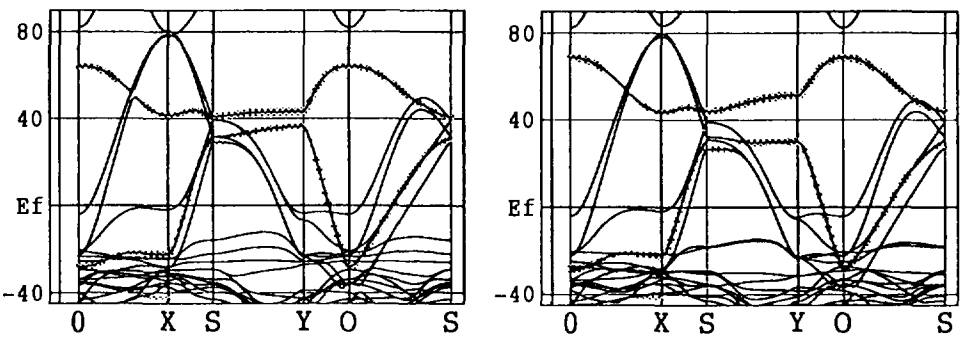

(a) (b)

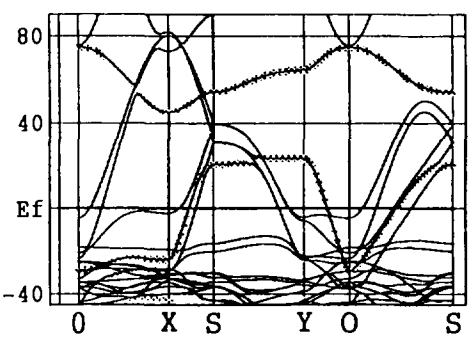

(c)

Figure 3: Effect of zone-boundary displacements on the band structure. The displacement patterns are alternating along the chain with a doubled unit cell. Two chain bands appear from folding in the previous single one. They are marked in the panels.
a) Apex oxygen displacement in z-direction, alternatingly up and down, $u = \pm 0.1$Å is the sign-alternating change in oxygen–oxygen distance.
b) Chain oxygen displacement in y-direction, $v = \pm 0.1$Å is the alternating change in Cu–O bond length.
c) Simultaneous displacement as in a) by $u = \pm 0.075$Å and as in b) by $v = \pm 0.15$Å.

One can see from Fig. 2 and Fig. 3 that the chain oxygens produce by far the strongest deformation potentials for the antibonding chain band. It is, however, interesting to note that the influence of z-displacements of plane-Cu, plane-O, and also of Ba on the chain band is not symmetric. Displacements towards the chain and away from it produce amplitudes of band deformation, very different in absolute value. This results in a dependence of the average occupation of the chain band, that is, of the doping parameter δ, on the amplitude of those vibrations. A consequence may be a contribution to the isotope effect on T_c via an isotope effect on δ. This contribution to the isotope effect on T_c would be weakest at optimal doping, where the influence of δ on T_c is weakest [6].

Our results for the model parameters are

$$\begin{aligned} E_1 &= 2\text{eV} - 1.76\text{eV/Å} \cdot u + 0.55\text{eV/Å} \cdot v, \\ E_2 &= 0 - 0.88\text{eV/Å} \cdot u + 0.55\text{eV/Å} \cdot v, \\ T &= 1.70\text{eV} - 1.23\text{eV/Å} \cdot u - 1.60\text{eV/Å} \cdot v, \end{aligned} \tag{5}$$

where u is the change in the vertical distance of the two apex oxygens from each other, and v is the change in chain-Cu–chain-O bond length. These numbers fit simultaneously the results of Fig. 2a and of Fig. 3. The other modes, producing much weaker band deformations, were not considered further.

5. Screened Coulomb Interaction

As a next step, we generalize the Hamiltonian (3) by introducing Coulomb correlation terms according to

$$\hat{H} = \sum_{<ij>} h_{ij}(\boldsymbol{u}) \hat{c}_i^\dagger \hat{c}_j + \sum_{<ij>} U_{ij}(\boldsymbol{u}) \hat{c}_i^\dagger \hat{c}_i \hat{c}_j^\dagger \hat{c}_j, \tag{6}$$

where the sums are over on-site and nearest-neighbour contributions, and the first sum is a short notation of (3). In order to obtain the Coulomb matrix element U for our CuO_2 molecular orbital we started from atomic values $U_d = 8\text{eV}$, $U_p = 2.5\text{eV}$, and $V_{dp} = 1.3\text{eV}$ for the Cu-d orbital, the O-p orbital, and the nearest-neighbour interaction matrix element, respectively. Those are characteristic values used in the literature.

The molecular orbital of Fig. 1 is a linear combination

$$\phi = c_d(u)\phi_d + c_p(u)(\phi_{p1} - \phi_{p2}) \tag{7}$$

of the copper-d state and the apical oxygen-p states. Using the above U's and V, and coefficients $c(u)$ obtained from our model (3), we get

$$\begin{aligned} U_{11} &= 4.5\text{eV} + 1.5\text{eV/Å} \cdot u, \\ U_{22} &= 2.5\text{eV}, \\ U_{12} &= 1.3\text{eV} - 1.3\text{eV/Å} \cdot v. \end{aligned} \tag{8}$$

The last deformation potential with respect to v is a guess. The subscript 1 stands for the CuO_2 radical and 2 stands for the chain oxygen atom. Spin indices are suppressed here, while in (6) i and j denote both chain site and spin.

6. CDW Groundstate and Excitations

The Hartree-Fock groundstate of (6) is a Slater determinant of single-particle spin-orbitals

$$\psi_\mu(\boldsymbol{r}) = \sum_i c_\mu^i \phi_i(\boldsymbol{r}). \tag{9}$$

Here, i again denotes both chain site and spin. The corresponding single-particle spin-density matrix is

$$P_{ij} = \langle \hat{c}_i^\dagger \hat{c}_j \rangle = \sum_\mu^{\text{occ.}} c_\mu^{i*} c_\mu^j. \tag{10}$$

We use the following expression for the total energy of a frozen deformation pattern:

$$E_{\text{tot}} = \sum_{ij} P_{ij} h_{ij}(\boldsymbol{u}) + \sum_{ij} P_{ii} U_{ij}(\boldsymbol{u}) P_{jj} - \sum_{ij} |P_{ij}|^2 U_{ij}(\boldsymbol{u}) + E_{\text{MP2}} + \frac{1}{2} \sum_{i\nu} K_{i\nu} u_{i\nu}^2. \tag{11}$$

The first three contributions comprise the Hartree-Fock expectation value of (6). The fourth term denotes the second order Møller-Plesset perturbation contribution, and the last term is the elastic energy of the lattice, originating from direct ion–ion interaction and the energy of the valence electrons, except those of the chain band states. We determined the force constants $K_{i\nu}$ so that the experimental vibration frequencies of the corresponding zone-center modes are reproduced by the total energy expression (11). The obtained values are

$$K_u = 7.9\text{eV/Å}^2, \qquad K_v = 9.1\text{eV/Å}^2. \tag{12}$$

The deformation parameters u and v are those used in (5) and (8).

The parameters of the expression (11) are the c_μ^i of (9) and u and v. For finite chains of lengths typically of 60 to 100 formula units, and for given electron numbers, those parameters were varied iteratively to find the minimum of (11). The results are deformation patterns and charge distributions over the chain. In order to check the approximations of (11), we compared the results with direct diagonalization of (6) for short chains and found very close agreement.

Fig. 4 shows the deformation pattern and the CDW for an exactly quarter filled chain band. As expected, a Peierls distorted superstructure with a period of four original unit cells is obtained. The corresponding Peierls gap in the band is 1.2eV, but this number depends sensitively on U_{12} and its deformation potential. This CDW, which was predicted already in [1] by calculations on the basis of model (3), was recently directly seen by scanning tunneling microscopy [2]. (Note that the experimental period is very close to four unit cells, while for a strongly correlated situation considered in [7] a period of two unit cells should be expected.). Further

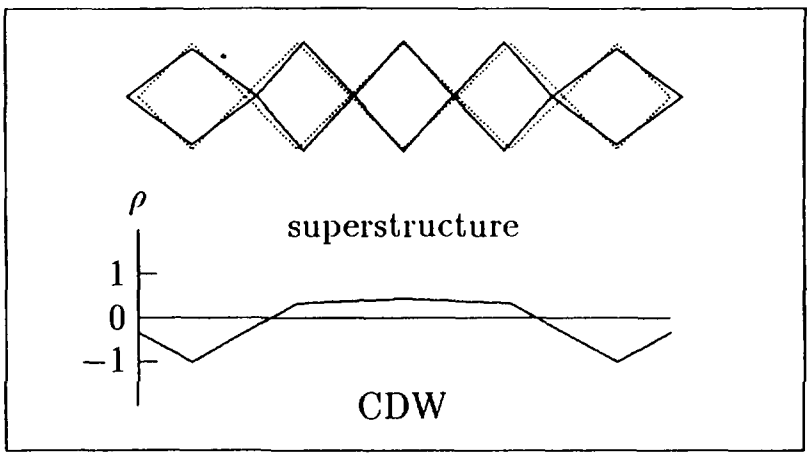

Figure 4: Deformation pattern and CDW of a quarter filled chain. The corners of the plaquettes are the oxygen positions (true scale). Dotted lines give the undistorted chain. The charge ρ per plaquette of the CDW is given in proton charge units.

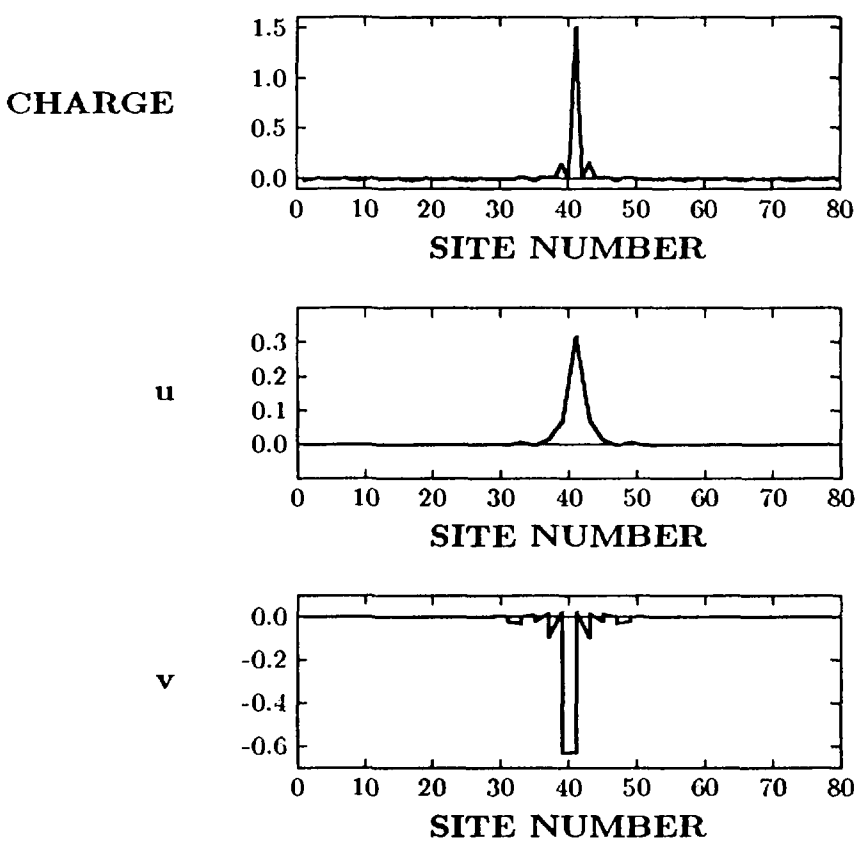

Figure 5: Excess charge distribution and deformation parameter changes of a hole bipolaron. Charge in proton charge units, deformation in Å.

experimental support of our CDW picture, involving large displacements of the chain oxygen, is provided by thermal diffuse scattering data [8] and x-ray-diffraction data [9]. In this context also difficulties to observe the longitudinal vibrations of chain oxygen off the zone center by inelastic neutron scattering [10] are noteworthy. The amplitude of displacements of the apical oxygens in c-direction is experimentally less clear. Relatively large split-positions of 0.13Å reported by EXAFS-studies [11] might be caused by chain oxygen vacancies affecting strongly the apex oxygen positions at the chain ends [12, 13].

Starting with the commensurate CDW groundstate we put additional electrons or holes into the chain and find their charge autolocalized in local deformation patterns extenting over a few formula units. A rich variety of such solutions is found with formation energies (differences of results for (11) with additional particles taken from the Fermi level) of a few tenths of an eV and hence deep in the Peierls gap. There are electron and hole polarons, electron and hole bipolarons, solitons, neutral polarexcitons, and others. An example of a hole bipolaron is given in Fig. 5.

7. Conclusions

One-dimensional structure elements are either present in the primary structure of cuprates as in $YBa_2Cu_3O_7$, or appear as low temperature structural modulations [14]. If a quasi-onedimensional band is singled out in the vicinity of the Fermi level, a CDW is very likely forming due to the large oxygen deformation potentials arising from the large polarizability of the O^{-2}-ion.

The Peierls gap of the commensurate CDW is filled with nonlinear polaronic excitations of both fermionic (e.g. polarons) and bosonic (e.g. bipolarons) type. The chemical potential is expected to adjust within the density of states of those polaronic excitations, because charge shifts are connected with those excitations producing Madelung potential terms.

Bipolarons may form heavy scattering centers for conduction holes of the cuprate planes. They also may mediate attraction between those conduction holes and hence contribute to the pairing mechanism of superconductivity [15, 16].

Acknowledgements

We would like to thank Prof. A. Müller and Prof. D. Mihailovic for useful discussions and the DFG under Grant No. Dre-269/1-5 for financial support.

References

1. H. Eschrig and S.-L. Drechsler, *Physica C* **173** (1991) 80; H. Eschrig, S.-L. Drechsler, and J. Malek, in *Phase Separation in Cuprate Superconductors* (Eds. K.A. Müller and G. Benedek, World Scientific Singapore 1993) p. 280.
2. H.L. Edwards et al., *Phys. Rev. Lett.* **73** (1994) 1154.
3. N. Nücker et al., *Phys. Rev. B* (submitted) (1994).
4. W.E. Pickett, R.E. Cohen, and H. Krakauer, *Phys. Rev. B* **42**, (1990) 8764.

5. O.K. Andersen et al., *Physica C* **185-189**, (1991) 147.
6. V.Z. Kresin and S.A. Wolf, *Phys. Rev. B* **49** (1994) 3652; these Proceedings.
7. R. Fehrenbacher, *Phys.Rev.* **B 49** (1994) 12 230.
8. Y. Koyama and Y. Hasebe; *Phys.Rev. B* **37** (1988) 5831.
9. J.D. Sullivan et al., *Phys. Rev. B* **48**, (1993) 10 638.
10. W. Reichardt, these Proceedings.
11. J. Mustre de Leon et al., *Phys.Rev.Lett.* **65** (1990) 1675; E.A. Stern et al., *Physica C* **209** (1993) 331.
12. T. Egami et al., in *Electronic Structure and Mechanisms of High-Temperature Superconductivity*, ed. J. Ashkenazi et al. (Plenum Press, N.Y., 1993); these Proceedings.
13. J. Röhler, these Proceedings.
14. A. Bianconi, these Proceedings.
15. J. Ranninger, *Z. f. Phys. B* **84** (1991) 167; these Proceedings.
16. Y. Bar-Yam, *Phys.Rev.* **B 43** (1991) 359.